Article

NDI-induced Topological Conversion of Human Telomeric G-Quadruplexes from Hybrid-2 to Parallel Form

HAO Xueyu[1,2], LI Chunjie[1], WANG Yu[1,2], ZHANG Feng[1], HOU Jingwei[1], KANG Chunqing[1,2]✉ and GAO Lianxun[1]

Received January 15, 2021
Accepted February 9, 2021

G-Quadruplexes(GQs), which are formed by G-rich DNA sequences in human telomeres, have become an attractive target for cancer treatment. The ligands to stabilize the conformation of human telomeric GQs *in vivo* are particularly important for structure-based ligand design and drug development targeting the noncanonical DNA structure. Here we report the conformational conversion of Tel26 induced by a naphthalene diimide(NDI) ligand in K^+ buffer, even at cellular physiological temperature(37 °C) and under mimetic cellular crowding conditions created by Ficoll 70. We provide an insight into the dynamic conversion from initial hybrid-2 GQ topology to final parallel GQ topology. These results are helpful for the design of ligands with GQ conformation regulation.

Keywords G-Quadruplex; Naphthalene diimide; Topological conversion; Telomeric DNA

1 Introduction

G-Quadruplexes(GQs) are a noncanonical four-stranded DNA structure formed by guanine(G)-rich repeat sequences through Hoogsteen hydrogen bonding in the presence of monovalent cations, such as K^+ and Na^+[1]. GQs are widespread in human genome and have gained attention in recent years owing to their critical roles in the regulation of cancer growth and proliferation[2−6]. Diversified GQ topologies are identified depending on the sequence, strand orientation, and conformation of loops formed by the bases between guanines. The GQs formed by human telomeric DNA sequences usually adopt hybrid-1 or hybrid-2 topology in K^+ solution(Fig.1)[7], while slight variations in the sequences can result in different GQ topologies. The loop arrangements and strand orientations are different between the two hybrid structures. For example, the 23-nt telomeric sequence(Tel23) d[TAGGG(TTAGGG)$_3$] is folded into hybrid-1 topology, whereas 26-nt telomeric sequence(Tel26) d[TTAGGG(TTAGGG)3TT] is hybrid-2 topology[7,8]. In addition, GQ topology is sensitive to cation species, ligands, crowding agents and other surrounding environmental factors. Some ligands can selectively target and stabilize human telomeric GQs[9—12] and even induce topological conversion of the GQs[9,13]. Previous studies also demonstrated the conformational conversion of the GQs from hybrid to parallel topology in molecular crowding environment created by PEG[14−17], but not by Ficoll 70[18].

Naphthalene diimide(NDI) ligands can stabilize GQs with exceptional affinity for G-quadruplex owing to the large π-planar aromatic surface[5,6,19]. Previous studies have demonstrated that the stabilization of GQ structure with NDI ligands can regulate cellular processes including cell cycle and apoptosis, showing the potential of NDIs in cancer treatments[5,6]. Recently, we found that NDI ligands can induce the conformational conversion of human telomeric GQs from an initial hybrid-1 topology to a final parallel topology in K^+ buffer[20]. To gain deep insights into the differences in the conformational conversion of two hybrid topologies, we moved to the topological transformation process of hybrid-2 GQ structure of Tel26. In this work, the induced conversion of Tel26 by NDI ligand S4 can be processed either at cellular physiological temperature(37 °C) or under mimetic cellular crowding conditions created by Ficoll 70, which is the same as that of Tel23. However, tracking the conformational changes

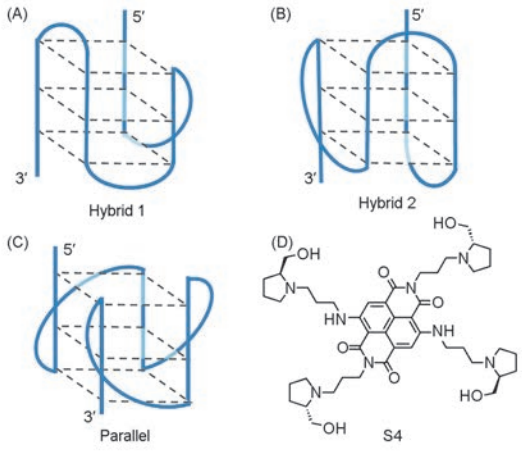

Fig.1 Schematic illustration of GQ and NDI ligand structures
(A) Hybrid-1; (B) hybrid-2; (C) parallel GQ structure; (D) S4 structure.

✉ KANG Chuanqing
kangcq@ciac.ac.cn
1. Laboratory of Polymer Composite and Engineering, Changchun Institute of Applied Chemistry, Chinese Academy of Sciences, Changchun 130022, P. R. China;
2. University of Science and Technology of China, Hefei 230026, P. R. China

https://doi.org/10.1007/s40242-021-1022-9

with fluorescence probes reveals the differences in unfolding and folding of the GQs in the two subtype of hybrid topologies. Here we report the details.

2 Experimental

2.1 DNA Oligonucleotides and NDI Ligand S4

Tel26[5′-TTAGGG(TTAGGGA)$_3$TT-3′] used in this study was purchased from Comate(Changchun, China). DNA oligonucleotides substituted with 2-Ap(2-aminopurine) or labeled with 6-carboxy-fluorescein(FAM) at 3′-terminal[5′-TTAGGG(TTAGGGA)$_3$TT-FAM-3′] were purchased from Sangon Biotech(Shanghai, China). The concentrations of DNA oligonucleotides were calculated from absorbance and extinction coefficient at 260 nm. The NDI ligand S4 was prepared in the same procedures as previous report[20].

Tel26 DNA samples were prepared according to previous report[20]. For RTM25, Tel26 was annealed by incubating at 95 °C for 10 min and then slowly cooled to room temperature (25 °C) followed by incubation at 4 °C overnight. S4 ligand was added to Tel26 samples at 25 °C for a while before the measurement. For RTM37, Tel26 was annealed as mentioned above of RTM25. However, S4 ligand was added to DNA samples at 37 °C for 48 h before measurement. For CA95, a mixture of Tel26 and S4 ligand in buffer was co-annealed as mentioned above of RTM25 before it was recovered to room temperature and directly used for measurements. Buffers were used in this study containing 10 mmol/L Tris-HCl, pH 7.0, 1 mmol/L EDTA with 100 mmol/L KCl in the absence or presence of Ficoll 70(Sigma-Aldrich, USA). The buffer mimicked the intracellular salt environment containing 25 mmol/L HEPES, pH 7.5, 10.5 mmol/L NaCl, 110 mmol/L KCl, 130 nmol/L $CaCl_2$, 1 mmol/L $MgCl_2$, 1 mmol/L DTT and Ficoll 70.

2.2 Circular Dichroism Spectroscopy

Circular dichroism(CD) spectra were collected from 220 nm to 320 nm on a Bio-Logic MOS-450(BioLogic Science Instruments, France) spectrometer in a 0.1-cm path length cuvette with a 2-nm bandwidth and 0.5-s response time. A digitalized thermostatic bath with CD instrument was used to balance the temperature in temperature-varying experiments.

2.3 Fluorescence Spectroscopy

The fluorescence spectra were recorded on a Perkin Elmer FL6500(PerkinElmer Life Sciences, USA) spectrometer. The emission spectra of 2-Ap-substituted DNA oligonucleotides were collected from 320 nm to 420 nm with the excitation at 305 nm. The fluorescence spectra of FAM-labelled Tel26 were collected from 507 nm to 800 nm with the excitation at 492 nm.

3 Results and Discussion

3.1 Topological Conversion of Hybrid-2 Type G-Quadruplex

Three protocols were used for the preparation of Tel26 samples(RTM25, RTM37 and CA95). As shown in Fig.2(A), the CD spectra of free Tel26 show a negative peak near 240 nm and a positive peak near 290 nm with a shoulder peak at 266 nm, which was consistent with the typical pattern of hybrid GQ(hGQ) topology in K^+ buffer[21]. And no sensible changes of CD signals were observed after binding with S4 through RTM25. However, there were significant changes in CD spectra of S4-Tel26 mixture prepared through CA95 with the disappearance of the peak at 290 nm and the emergence of a new positive peak at 266 nm. The induced CD spectra were consistent with the parallel GQ(pGQ) topology, which indicated the conformational conversion of Tel26 from hybrid to parallel topology induced by S4. The same induced CD spectra were also observed for S4-Tel26 mixture prepared through the incubation at physiological temperature(37 °C) for 48 h(RTM37) in the presence or absence of Ficoll 70 that was used to mimic cellular crowding conditions[Fig.2(B) and (C)]. These results unambiguously indicated that the hGQ of Tel26 transformed to pGQ by co-annealing or long-term incubation at the biological temperature but not by S4 binding at 25 °C.

The thermal stability of induced pGQ by S4 was studied by temperature-varying experiments. During the temperature increasing up to 90 °C, the CD signal of induced Tel26 pGQ at 266 nm remained intact[Fig.2(D)], whereas no CD signal reserved for free Tel26[Fig.2(E) and (F)]. These results confirmed that NDI-induced pGQs were more stable than the hGQ precursors, which was consistent with the previous study that substituted NDI compounds binded selectively to pGQ[22].

To further understand the transformation process, dynamically monitoring S4-Tel26 mixture during the incubation at 37 °C within 48 h was conducted by CD spectrometry. As shown in Fig.2(G), slow and continuous changes of the CD signals were observed with a decrease at 290 nm and an increase at 266 nm along with time. The results confirmed that the configurational transformation of Tel26 induced by S4 was a dynamic process from hybrid-2-type GQ to pGQ like that of Tel23[20], though the sequences had different hybrid topologies. The trend of the CD signals at 266 and 292 nm *vs*. time reached to stable states after 24 h when the topological conversion completed[Fig.2(H)]. Tel26 is faster in the topological conversion than Tel23 that requires about 36 h[20]. The differences between two different GQ hybrid topologies might affect the

https://doi.org/10.1007/s40242-021-1022-9

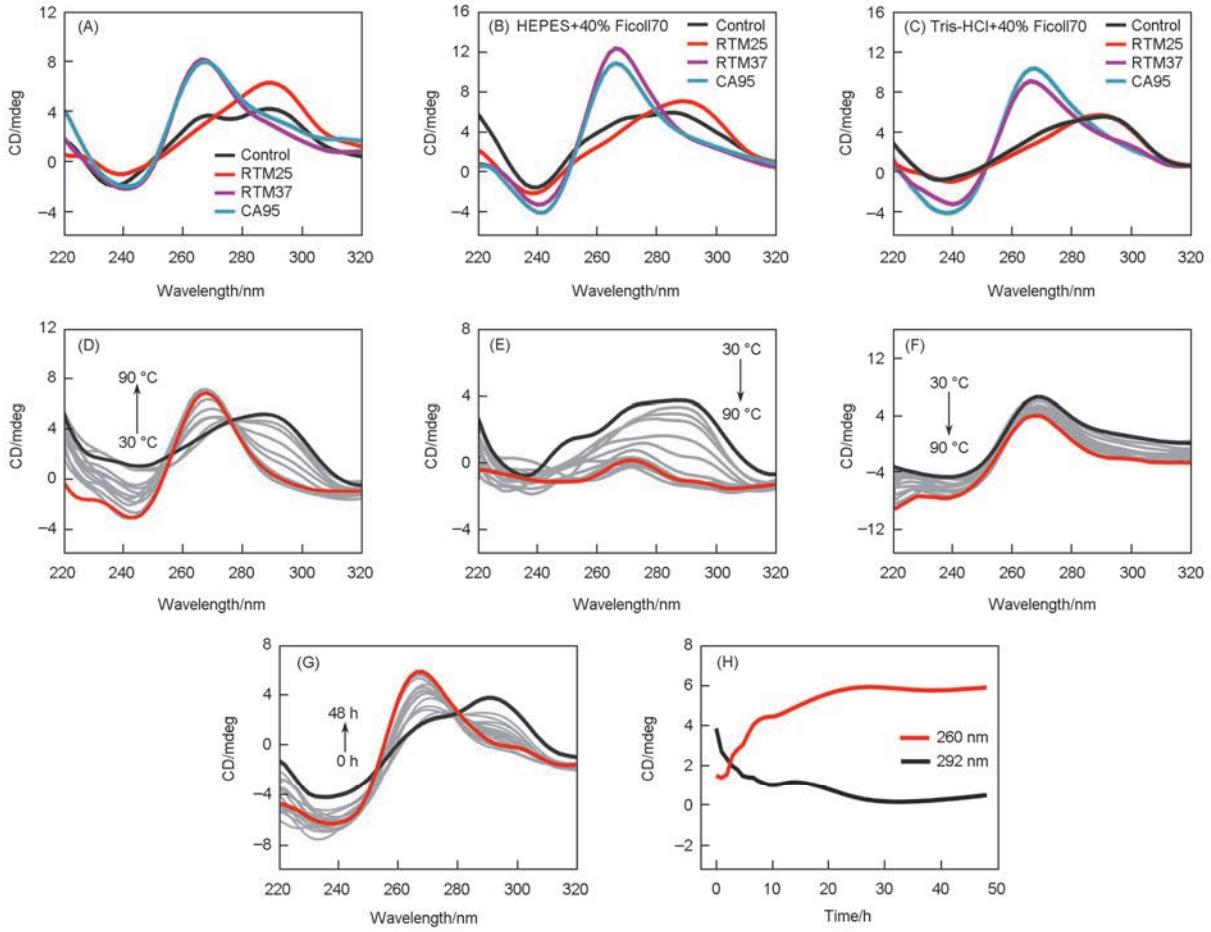

Fig.2 CD spectra of Tel26

(A) CD spectra of Tel26(10 μmol/L) binding with S4(30 μmol/L) through RTM25, RTM37 and CA95 in Tris-HCl buffer; Tel26 binding with S4 through RTM25, RTM37 and CA95 under molecular crowding condition created by addition of 40% Ficoll70 in HEPES buffer(B) and Tris-HCl buffer(C) containing 110 mmol/L KCl. No ligand presents in control experiments; CD spectra of Tel26 binding with S4 through RTM25(D), free Tel26(E) and S4-Tel26 mixture(F) through CA95 followed by heating to 90 °C in Tris-HCl buffer; (G) CD spectra of Te26 binding with S4 *vs*. time in Tris-HCl buffer at 37 °C(from 0 h in black to 48 h in red); (H) the trend of CD signals at 266 nm(red) and 292 nm(black) along with time, drawn according to (G).

kinetics of configurational transformation induced by NDI-ligand.

3.2 Conformational Transformation of TTA Loops During the Topological Conversion of Hybrid-2-type GQ

2-Aminopurine(Ap) is a fluorescent adenine analogue and has been used to probe the conformational changes in DNA[15,17]. Substitution of adenine in Tel26 with Ap was used to further study the conversion process[Fig.3(A)]. The fluorescence spectra of free Tel26^{Ap} sequences showed different intensities owing to the TTA loop conformational heterogeneity[Fig.3(B)]. Upon binding with S4 through RTM25 and CA95, the considerable fluorescence quenching of Tel26^{Ap3} has been observed with the same quenching degree[Fig.3(C) and (D)]. We speculate that the change in fluorescence intensity under RTM25 condition is caused by the association of S4 with Tel26 at 5′-terminal end-stacking, not the conformational conversion. Owing to the different environments of TTA loops in Tel26 hGQ, the different fluorescence intensities of Tel26^{Ap9}, Tel26^{Ap15} and Tel26^{Ap21} were observed after binding with S4 through RTM25. However, the fluorescence intensities of Tel26^{Ap9}, Tel26^{Ap15} and Tel26^{Ap21} were closer after processed through CA95, which was consistent with structural symmetry of the TTA loops in induced Tel26 pGQ[Fig.3(A)]. The relative change in fluorescence intensities of the Tel26^{Ap} samples from hGQ to pGQ followed the order of Ap15>Ap9>Ap21>Ap3[Fig.3(E)]. It was inconsistent with the order of Tel23^{Ap}, Ap14>Ap20>Ap8>Ap2[20]. The inconsistence between Tel26 and Tel23 reflected the subtle difference in the location transition of the TTA loops of the sequences during the topological conversion. Both Ap3 in Tel26^{Ap3} and Ap2 in Tel23^{Ap2} were located in 5′-end of the sequences and had minimum change in fluorescence intensity on the topological conversion, which indicated the binding of S4 at 5′-terminal[23,24]. The lateral TTA loops containing Ap15 and Ap9 in Tel26 hybrid-2 GQ and those containing Ap14 and Ap20 in Tel23 hybrid-1 GQ showed relative large variation in

https://doi.org/10.1007/s40242-021-1022-9

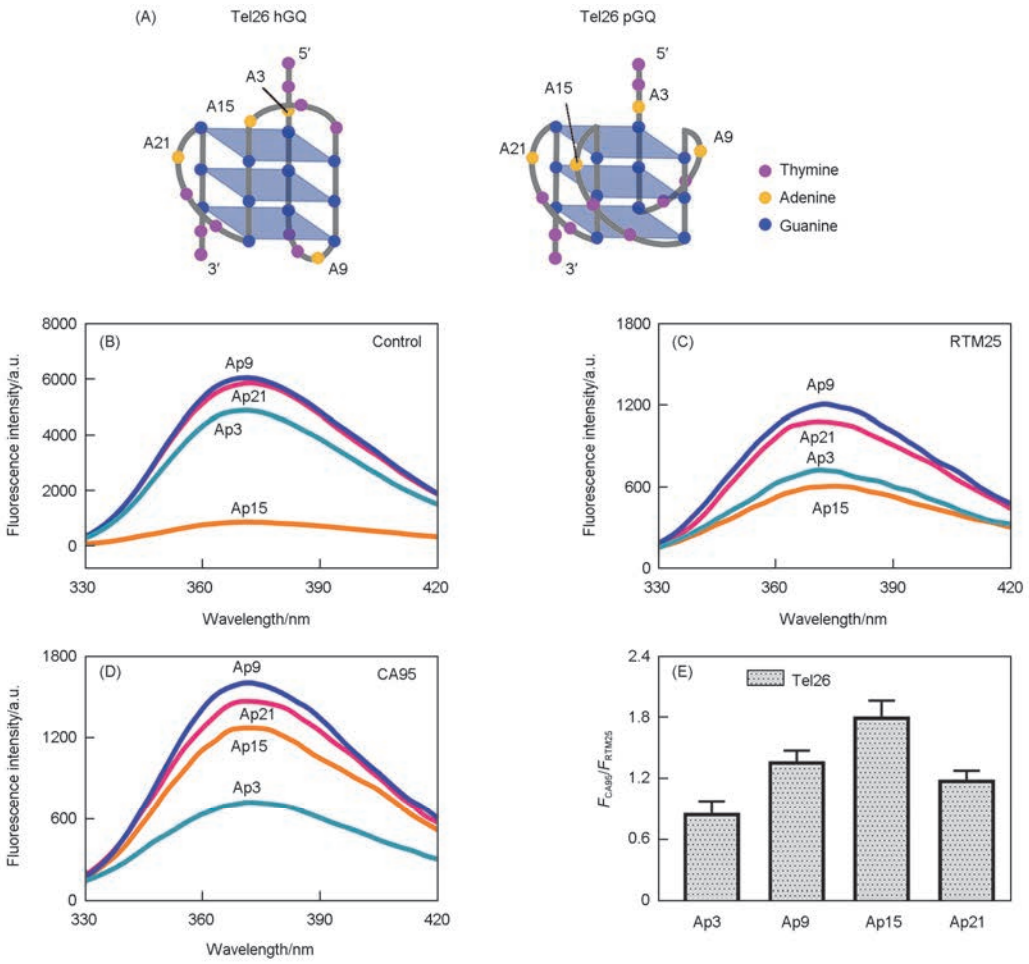

Fig.3 Fluorescence analysis of 2-aminopurine(Ap) substituted at different adenine residues in Tel26

(A) Schematic illustration of adenine residues in two types of Tel26 GQ structures; fluorescence spectra(λ_{ex}=305 nm) of free Tel26(B), hybrid-(C) and parallel-type(D) S4-Tel26 mixture though RTM25 and CA95, respectively; (E) fluorescence analysis of Ap substituted in S4-Tel26 mixture though RTM25 and CA95, respectively. F_{CA95} and F_{RTM25} are the emission fluorescence intensities at 370 nm, respectively.

the fluorescence intensities on transferring to propeller TTA loops.

3.3 Dynamic Process of Topological Conversion of Hybrid-2 Type GQ

FAM-labelling is usually used to detect the interaction between ligand and DNA[25]. Considering the overlap between the emission spectra of FAM and the excitation spectra of S4 ligand, we choose FAM as a donor labeled on the 3′-end of Tel26 to investigate the conformational conversion process that leads to changes in the distance between FAM and S4 and thus Förster resonance energy transfer(FRET) efficiency. S4-Tel26-FAM mixture was incubated at 37 °C and monitored by fluorescence spectrometry for 48 h. As shown in Fig.4(A) and (B), the fluorescence intensities at 520 nm (emission of FAM) gradually enhance while those at 652 nm (emission of S4) gradually quench along with time and both reach stable after 20 h, which indicates that FAM at the 3′-end of Tel26 has changes in chemical microenvironment during the conformational conversion. We propose that the formation of unfolded GQ intermediate states leads to a change in the distance between FAM and S4. However, the recovery did not arise after the topological conversion. The previous study has showed efficient charge transport through G-quadruplex[26]. Therefore, we speculate that the unrecovery of the fluorescence intensity may be due to the difference of energy transfer efficiency between hybrid and parallel topologies.

To further verify the Tel26 topological conversion, the continuous fluorescence analysis of Tel26^{Ap} samples during the incubation at 37 °C for 48 h revealed the kinetic conformational conversion of Tel26[Fig.4(C)—(F)]. The fluorescence intensity of S4-Tel26^{Ap} mixtures changed rapidly during the initial hours due to the changes in the environment around Ap after binding with S4 ligand. Subsequently, the fluorescence intensities of Tel26^{Ap3} and Tel26^{Ap9} tended to be stable after 10 h, and those of Tel26^{Ap15} and Tel26^{Ap21} stabilized after 24 h and 36 h, respectively. The relatively rapid fluorescence fluctuation of Tel26^{Ap3} and Tel26^{Ap21}, in which Aps were located at 5′-end of Tel26 hGQ, within the initial phase was attributed

https://doi.org/10.1007/s40242-021-1022-9

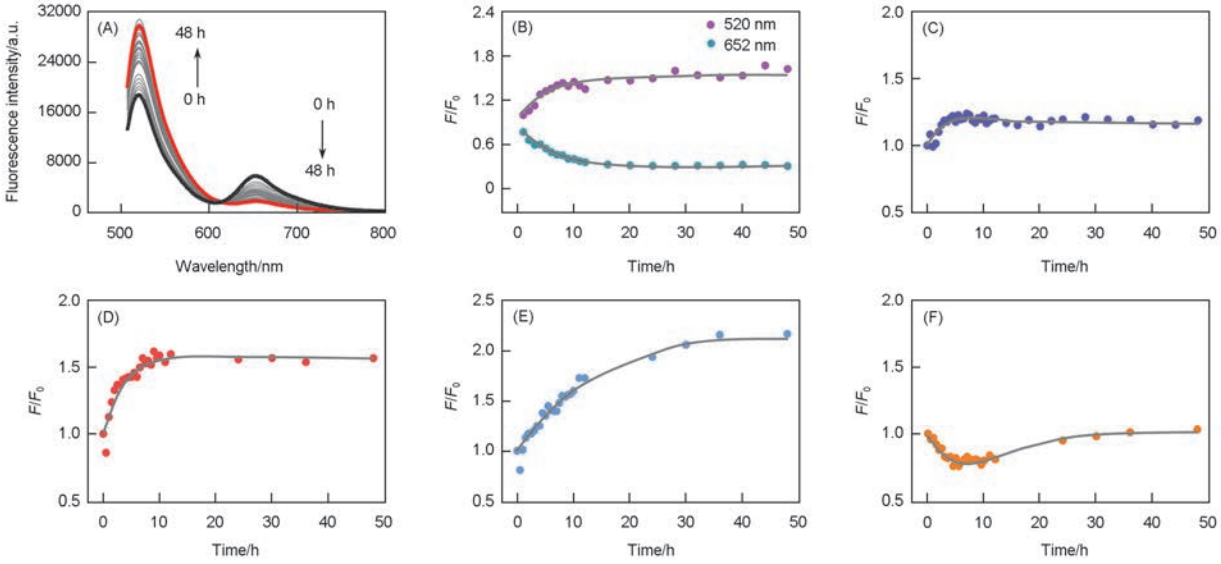

Fig.4 Dynamic topological conversion of Tel26

(A) Time-dependent fluorescence spectra(λ_{ex}=492 nm) of S4-Tel26-FAM mixture prepared from RTM37; (B) emissions of FAM(λ_{em}=518 nm) and S4(λ_{em}=656 nm) *vs*. time derived from (A); fluorescence spectra of S4-Tel26^{Ap3}(C), S4-Tel26^{Ap9}(D), S4-Tel26^{Ap15}(E) and S4-Tel26^{Ap21}(F) mixture at 37 °C during 48 h(λ_{ex}=305 nm, λ_{em}=370 nm). F_0 and F are the fluorescence intensities of samples at 0 h and different incubation time, respectively.

to the initiation of unfolding of Tel26 hGQ after the stacking of S4 on the 5′-terminal of Tel26. We observed that the fluorescence intensity of Tel26^{Ap21} after 24 h was similar to that at 0 h, indicating that the conformational conversion had little effect on the propeller TTA loop containing Ap21. The loop remained at the propeller location during the topological conversion. The topological conversion process caused the great change in the fluorescence intensity of Tel26^{Ap9} and Tel26^{Ap15}. Continuous change in the fluorescence intensity of Tel26^{Ap15} was observed during the entire incubation period. The fluorescence intensities of Tel26^{Ap9} and Tel26^{Ap15} reached stable after 36 h, which was reasonable to indicate that the TTA loops of Tel26^{Ap9} and Tel26^{Ap15} transformed throughout the conformational transformation. The stabilization of the fluorescence intensities of Tel26^{Ap} samples indicated that the configuration was no longer changing and reached to the stable hGQ. The fluorescence changes observed in Tel23^{Ap} samples and Tel26^{Ap} samples had a certain difference, which might be caused by the influence of the difference between the two hybrid-type GQ structures on the conformational conversion.

3.4 Mechanistic Consideration of Topological Conversion

The conformation of Tel26 was hGQ at 25 °C in K^+ buffer, and S4 interacted with Tel26 at 5′-terminal by an end-stacking binding model[Fig.5(A)], which was consistent with the previous studies[23,24]. However, the stacking interaction between the extended planar heteroaromatic surface of NDI-ligand and the 5′-terminal of hGQ could cause steric hindrance of the ligand with the 5′-end and TTA loop at the 5′-terminal of hGQ, consisting with the relatively rapid fluctuation of Tel26^{Ap3} and Tel26^{Ap21} with Aps located at the 5′-terminal of hGQ(Fig.4). At physiobiological temperature (37 °C), the steric hindrance led to the configuration distortion of Tel26 hGQ after binding with S4 ligands. In the presence of S4, the distorted hGQ gradually unfolded through a dynamic process as shown by the gradual emergence of the CD signal at 266 nm and the disappearance of the CD signal at 290 nm in the CD spectra along with time[Fig.2(G)]. Unfolded forms of G-rich DNA(G-hairpin, G-triplex, etc.) have been considered as common intermediates produced in the topological conversion[27—31].

According to the results and related literature, we speculate the mechanism of the topological conversion of Tel26 GQ with the hybrid-2 topology in Fig.5. Tel26 hGQ may change in configuration distortion to accommodate interaction with S4 to form intermediate states[Fig.5(B) and (E)], which is consistent with rapid change in fluorescence intensities of Tel26^{Ap3} and Tel26^{Ap21} in the initial phase[Fig.4(C) and (F)]. During the conformational conversion process, Tel26 hGQ with distorted configuration may first unfold from the middle strand, and then the strand at 5′-terminal to form the intermediate states[Fig.5(C) and (D)] according to the gradual increase in the fluorescence intensity of Tel26^{Ap15}[Fig.4(E)] and fluorescence change of Tel26^{Ap3}[Fig.4(C)]. Because of the difference between the two types of hybrid structure, the order in strand unfolding is quite different, in which Tel23 unfolds from the strand from 3′-terminal[20]. Subsequently, the

https://doi.org/10.1007/s40242-021-1022-9

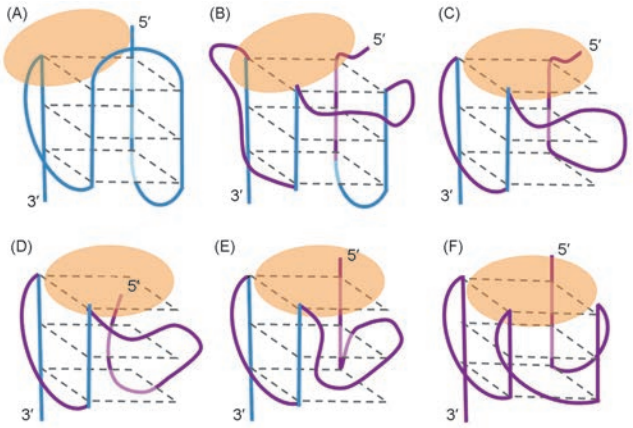

Fig.5 Proposed mechanism of the topological transformation of Tel26 from hybrid-2 GQ(A) to parallel GQ(F) at physiological temperature(37 °C) in K^+ buffer with intermediate states(B—E)

unfolded strands adjust the orientation according to the S4 binding site, and reform Tel26 pGQ, an ordered and stable topology[Fig.5(E) and (F)].

4 Conclusions

In summary, we have studied the dynamic conformational conversion of Tel26 from initial hybrid-2 GQ topology to final parallel GQ topology in K^+ buffer. The topological conversion is effective at cellular physiological temperature(37 °C) under mimetic cellular crowding conditions created by Ficoll 70. Due to the difference between hybrid-1 and hybrid-2 GQ structure (Fig.1), the topological transformation process of Tel26 is different from that of Tel23 in K^+ buffer. The results demonstrate an accurate regulation of the conformational conversion in GQs of DNA with different noncanonical folding topologies, which will be helpful in the design and construction of DNA-based functional nano-systems. Moreover, multiple conformations of telomeric GQs present under cellular conditions. The induced conversion from metastable hybrid-type GQs to stable parallel-type GQs suggests potential of NDI ligands in enhanced inhibition of telomerase activity. Forwarding research in the induced conformation of telomeric GQs in cell will be helpful for deeply understanding the interactions between NDI ligands and GQs and developing ligands with enhanced inhibition of cancer cell proliferation. The works are in progress in our laboratory.

Acknowledgements

The authors appreciate the technical help of Mr. LI Haoyu(Changchun Institute of Applied Chemistry, Chinese Academy of Sciences) for insightful comments and suggestions.

Conflicts of Interest

The authors declare no conflicts of interest.

References

[1] Williamson J. R., Raghuraman M. K., Cech T. R., *Cell*, **1989**, *59*(5), 871
[2] Jerry W. S., Woodring E. W., *Nat. Rev. Genet*., **2019**, *20*(5), 299
[3] Zhou X., Xing D., *Chem. Soc. Rev*., **2012**, *41*(13), 4643
[4] Ruggiero E., Richter S. N., *Nucleic Acids Res*., **2018**, *46*(7), 3270
[5] Ahmed A. A., Marchetti C., Ohnmacht S. A., Stephen N., *Sci. Rep*., **2020**, *10*(1), 12192
[6] Ahmed A. A., Angell R., Oxenford S., Worthington J., Williams N., Barton N., Fowler T. G., OFlynn D. E., Sunose M., McConvile M., Vo T., Wilson W. D., Karim S. A., Morton J. P., Neidle S., *ACS Med. Chem. Lett*., **2020**, *11*(8), 1634
[7] Zhang Z., Dai J., Veliath E., Jones R.A., Yang D., *Nucleic Acids Res*., **2010**, *38*(3), 1009
[8] Dai J., Carver M., Punchihewa C., Jones R. A., Yang D., *Nucleic Acids Res*., **2007**, *35*(15), 4927
[9] Lin C., Wu G., Wang K., Onel B., Sakai S., Shao Y., Yang D., *Angew. Chem. Int. Ed*., **2018**, *57*(34), 10888
[10] Liu W., Zhong Y., Liu L., Shen C., Zeng W., Wang F., Yang D., Mao Z., *Nat. Commun.*, **2018**, *9*, 3496
[11] Barthwal R., Raje S., Pandav K., *Bioorg. Med. Chem*., **2020**, *28*(23), 115761
[12] Yu Q., Wang M., *Bioorg. Med. Chem*., **2020**, *28*(17), 115641
[13] Wang Z., Li M., Chen W., Hsu S., Chang T., *Nucleic Acids Res*., **2016**, *44*(8), 3958
[14] Xu L., Feng S., Zhou X., *Chem Commun*., **2011**, *47*(12), 3517
[15] Xue Y., Kan Z. Y., Wang Q., Yao Y., Liu J., Hao Y. H., Tan Z., *J. Am. Chem. Soc*., **2007**, *129*(36), 11185
[16] Heddi B., Phan A. T., *J. Am. Chem. Soc*., **2011**, *133*(25), 9824
[17] Xue Y., Liu J., Zheng K., Kan Z., Hao Y., Tan Z., *Angew. Chem. Int. Ed*., **2011**, *50*(35), 8046
[18] Hänsel R., Löhr F., Foldynová-Trantirková S., Bamberg E., Trantírek L., Dötsch V., *Nucleic Acids Res.*, **2011**, *39*(13), 5768
[19] Zuffo M., Guédin A., Leriche E., Doria F., Pirota V., Gabelica V., Mergny J., Freccero M., *Nucleic Acids Res*., **2018**, *46*(19), e115
[20] Hao X., Wang C., Wang Y., Li C., Hou J., Zhang F., Kang Q., Gao L., *Int. J. Biol. Macromol.*, **2021**, *167*, 1048
[21] Takahashi S., Yamamoto J., Kitamura A., Kinjo M., Sugimoto N., *Anal. Chem.*, **2019**, *91*(4), 2586
[22] Vo T., Oxenford S., Angell R., Marchetti C., Ohnmacht S. A., Wilson W. D., Neidle S., *ACS Med. Chem. Lett*., **2020**, *11*(5), 991
[23] Parkinson G. N., Cuenca F., Neidle S., *J. Mol. Biol.*, **2008**, *381*(5), 1145
[24] Mpima S., A Ohnmacht S. A., Barletta M., Husby J., Pett L. C., Gunaratnam M., Hilton S. T., Neidle S., *Bioorg. Med. Chem*., **2013**, *21*(20), 6162
[25] Guo Y., Chen J., Cheng M., Monchaud D., Zhou J., Ju H., *Angew. Chem. Int. Ed.*, **2017**, *56*(52), 16636
[26] Wu J., Meng Z., Lu Y., Shao F., *Chem. Eur. J*., **2017**, *23*(56), 13980
[27] Mashimo T., Yagi H., Sannohe Y., Rajendran A., Sugiyama H., *J. Am. Chem. Soc*., **2010**, *132*(42), 14910
[28] Li W., Hou X., Wang P., Xi X., Li M., *J. Am. Chem. Soc*., **2013**, *135*(17), 6423
[29] Marchand A., Gabeliaca V., *Nucleic Acids Res.*, **2016**, *44*(22), 10999
[30] Maleki P., Budhathoki J. B., Roy W. A., Balci H., *Mol. Gen. Genomics*, **2017**, *292*(3), 483
[31] Hou X., Fu Y., Wu W., Wang L., Teng F., Xie P., Wang P., Xi X., *Nucleic Acids Res*., **2017**, *45*(19), 11401